This is a repository copy of *Mobilities of Ti and Fe in disordered TiFe-BCC assessed from new experimental data*.

Article:

Salmasi, A., Graham, S.J. orcid.org/0000-0002-1296-1680, Galbraith, I. et al. (6 more authors) (2021) Mobilities of Ti and Fe in disordered TiFe-BCC assessed from new experimental data. Calphad, 74. 102300. ISSN 0364-5916

https://doi.org/10.1016/j.calphad.2021.102300

CALPHAD: Computer Coupling of Phase Diagrams and Thermochemistry 74 (2021) 102300

Contents lists available at ScienceDirect

Calphad

journal homepage: www.elsevier.com/locate/calphad

Short communication

Mobilities of Ti and Fe in disordered TiFe-BCC assessed from new experimental data

Armin Salmasi [a,*], Simon J. Graham [b], Iain Galbraith [b], Alexander D. Graves [b], Martin Jackson [b], Susanne Norgren [c,d], Dikai Guan [b], Henrik Larsson [a], Lars Höglund [a]

[a] Department of Materials Science and Engineering, KTH Royal Institute of Technology, SE-100 44, Stockholm, Sweden
[b] Department of Materials Science and Engineering, The University of Sheffield, Sir Robert Hadfield Building, Mappin Street, Sheffield, United Kingdom
[c] AB Sandvik Coromant R&D, SE-126 80 Stockholm, Sweden
[d] Department of Mech. Eng., Production & Materials Engineering, Lund University, 223 62 Lund, Sweden

ARTICLE INFO

Keywords:
Disordered BCC titanium iron
Mobility database
DICTRA
EPMA
Machining

ABSTRACT

Pure titanium has an HCP structure and lacks mechanical properties for many industrial purposes. The BCC phase of Ti is required to make alloys with increased strength compared to pure Ti. Iron is the most potent element for stabilising the BCC phase. However, the addition of Fe to Ti causes segregation issues during solidification, which can be avoided by diffusion-driven solid-state alloying. To predict the diffusion kinetics, the interaction mobility parameters of Ti and Fe in the disordered BCC phase of Ti are necessary. In this work, these parameters are optimised based on new experimental data from Ti-Fe diffusion couples produced by the Field Assisted Sintering Technology (FAST). Diffusion couples were held at 1173K and 1273K for one hour. High-resolution Fe concentration profiles are obtained from Electron Probe Micro Analyser (EPMA). Ternary mobility interaction parameters are assessed based on binary endmembers with a DICTRA sub-module, and results are compared to earlier assessments of mobilities of the disordered BCC TiFe system.

1. Background and motivation

The assessment of the four endmembers of the Ti-Fe system, i.e. the tracer and impurity diffusivities of Ti and Fe in Ti and Fe, are reported in Refs. [1,2]. Hence, re-assessment of the endmembers is not the aim of this work. On the other hand, Ti-Fe diffusion couple data leads to an accurate assessment of ternary interaction parameters. These interaction parameters, together with binary parameters, are pillars of the kinetic database that will be used to model the diffusion in Ti-Fe disordered BCC.

New experimental data has been obtained from Ti-Fe diffusion couples produced via field-assisted sintering technology (FAST).

FAST is a powder metallurgy technique commonly used for the consolidation of various materials, including metals [3]. This technique is suitable for producing diffusion couples as it is capable of high heating rates up to the desired diffusion temperature and applies a constant force for sustained contact between the different materials. An application of this is diffusion bonding of dissimilar Ti alloys by consolidating powders in layers, which has been investigated as an alternative to fusion welding, with the diffusion of alloying elements measured across the interfaces [4].

Diffusion in the Ti-Fe system is of interest for several reasons. Pure Ti is HCP and lacks the mechanical properties necessary for many industrial applications. On the other hand, the BCC-Ti phase is a more versatile alloy with increased strength compared to pure Ti. Fe is the most potent element for stabilising the BCC phase of Ti. Although Fe is a relatively low cost alloying addition, it is not greatly used due to segregation issues during solidification [5]. However, this can be avoided by alloying within the solid state. Therefore, understanding and prediction of diffusion kinetics aids in the production of homogeneous alloys from blended elemental powders. Fe is also known to exhibit very fast diffusion in Ti, i.e. the amount of diffusion necessary for homogenisation does not require excessive processing temperature or time [6]. Thermodynamic and kinetic modelling of systems like Ti-Fe can also improve understanding of tool wear in Ti alloy machining.

The interaction between the WC-Co tool and the workpiece governs the rate at which tools wear [7]. The diffusion of W, Co and C from the tool into Ti solid solution and the formation of reaction products such as TiC has been shown experimentally [8]. Such reaction products at the tool interface mediate diffusion driven tool degradation. Since there is a relationship between the relative BCC stability of Ti alloys and TiC

---

[*] Corresponding author.
E-mail address: salmasi@kth.se (A. Salmasi).

https://doi.org/10.1016/j.calphad.2021.102300
Received 18 March 2021; Received in revised form 22 May 2021; Accepted 30 May 2021

formation at the interface [9], the kinetic modelling of such tool-alloy systems is critical for the design of new tools and alloys.

As Fe is an extremely strong (and cheap) BCC-Ti stabiliser with a rapid diffusion rate and increasing viability in alloy development due to the use of powder metallurgy techniques [10–12], an accurate assessment is of immense practical value. The present work improves upon previous assessments of the Ti-Fe system, albeit limited to disordered BCC.

2. Experimental details

2.1. Production and analysis of Ti-Fe diffusion couples

10 g of commercially pure Grade 1 Ti powder (45-150 μm, Phelly Materials Inc. USA) was consolidated within a 20 mm diameter graphite mould via field assisted sintering using an FCT Systeme GmbH type HP D25 spark plasma sintering furnace. Parameters included a 100 K/min ramp rate to a dwell temperature of 1273 K, a 10 min dwell time and 35 MPa pressure. The surfaces of the resulting consolidated pellets were ground using silicon carbide grit paper up to P1200 to remove the graphite layer and give a flat surface for the diffusion couple. After a clean with isopropanol, the Ti pellets were then reinserted into the graphite mould, and 10 g of Fe powder (<60 μm, Goodfellow UK) was poured on top. The same FAST parameters were once again used, however, with two dwell temperatures of 1173 K and 1273 K, held for 60 min. The diffusion couples were then sectioned, ground and polished prior to analysis.

Elemental analysis across the resulting diffusion zone can be completed using electron probe microanalysis (EPMA). This technique is effective for this measurement due to the higher resolution compared with techniques like energy-dispersive X-ray spectroscopy (X-EDS). The resulting data is then plotted to give an element concentration profile across the interface for further diffusion analysis.

A JEOL JXA-8530F Plus was used to perform electron probe microanalysis (EPMA) across the interfaces and for backscattered electron (BSE) scanning electron microscopy. For EPMA, a scan line with step size of 1 μm and 250 μm length was measured, with 200 μm into the Ti and 50 μm into the Fe. An acceleration voltage of 20 keV was used for the BSE imaging.

3. Assessment procedure

3.1. Evaluation of tracer diffusivities $D_k^\star$ from database parameters

In this section the formulas are given for evaluating tracer diffusivities $D_k^\star$ from database parameters `MQ` and `MF`. The syntax for the parameters are of the form:

`MQ(<phase>&<diffusing element>,<colon separated list>;<order>)`

for both `MQ` and `MF`. The colon separated list of constituents run over all sublattices.[1] For an endmember, only one constituent (element) is given for each sublattice. For an interaction parameter, there will be two constituents listed on one sublattice. For an endmember, the “order” is always zero (and can optionally be excluded).

Note that here $D_k^\star$ designates tracer and impurity diffusivities and all compositions in between; the asterisk signifies a pure kinetic quantity, i.e. without the thermodynamic factor.

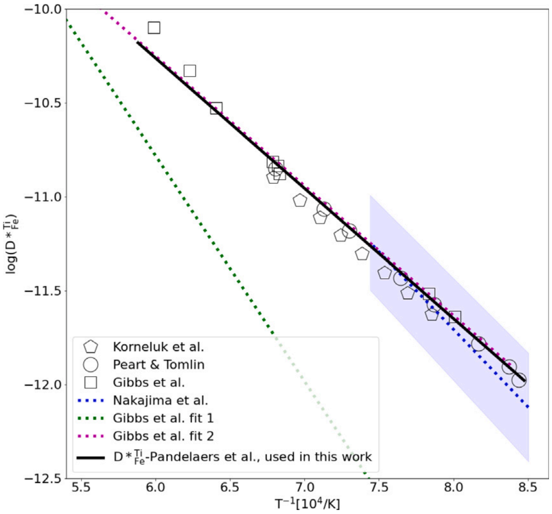

Fig. 1. Impurity diffusivity of Fe in BCC-Ti after [1,6,17–19].

3.1.1. Evaluating frequency factor and activation energy coefficients M_k^f and M_k^q from the parameters

Coefficients M_k^f and M_k^q are evaluated from the `MF` and `MQ` parameters respectively. Let Φ_k denote either M_k^f or M_k^q, then the expression is

$$\Phi_k = \sum_i x_i\,{}^{\circ}\Phi_{k,i} + \sum_i \sum_{j>i} x_i x_j \sum_{\nu=0}^{n} \left(x_i - x_j\right)^{\nu} \cdot {}^{\nu}\Phi_{k,ij} \tag{1}$$

where ${}^{\circ}\Phi_{k,i}$ denote an endmember and ${}^{\nu}\Phi_{k,ij}$ denote an interaction parameter of degree ν. The first term is thus a linear interpolation between the endmembers, and the second term, containing the interactions, is a Redlich–Kister series.

3.1.2. Evaluating $D_k^\star$ in ferromagnetic BCC from M_k^f and M_k^q

The model in Dictra [13] for diffusion in alloys with ferromagnetic ordering is due to Jönsson [14,15]. The expression for substitutional tracer diffusivities is

$$\mathrm{D}_k^\star = \exp\left(\frac{\mathrm{M}_k^f}{\mathrm{RT}}\right)\exp\left(\Lambda\alpha\xi\right)\exp\left(\frac{\mathrm{M}_k^q\left(1+\alpha\xi\right)}{\mathrm{RT}}\right) \tag{2}$$

For BCC alloys $\Lambda = 6$, $\alpha = 0.3$. The factor ξ is the ratio of the magnetic enthalpy at the current temperature and temperature zero, i.e.

$$\xi = \frac{{}^{mg}\Delta\mathrm{H}}{{}^{mg}\Delta\mathrm{H}(0)} \tag{3}$$

The magnetic enthalpies are determined by the thermodynamics of the system, viz. the Curie temperature T_C and the magnetic moment of BCC phase of Ti [16].

3.2. Endmember parameters in disordered BCC

The assessment by Jönsson et al. [14] of the tracer diffusivity of Fe is used in this work. A first degree linear fit to experimental data points reported in previous studies [6,17,18] is used to describe the Fe impurity diffusivity in Ti. This description is similar to the one suggested by Pandelaers et al. [1], as shown in Fig. 1.

A temperature dependent description of the activation energy of the tracer diffusivity of Ti is presented in Ghosh’s [20] summary of previous works [1,21–24].

Fitting higher degree expressions to the experimental data is not advantageous for modelling purposes. In the assessment of experimental data, the best practice is to reduce the number of parameters as much as possible to obtain the simplest description. Hence, in the present study, we use a linear fit to Ghosh’s assessment of the Ti tracer diffusivity.

---

[1] BCC has only two sublattices, and in this work, the only constituent of the second sublattice is the vacancy.

Table 1
Fe-Fe, Fe-Ti, Ti-Ti and Ti-Fe endmembers.

MQ(BCC_A2&FE; FE : VA)	−218000
MF(BCC_A2&FE; FE : VA)	$RT\ln\left(4.6\cdot10^{-5}\right)$
MQ(BCC_A2&FE; TI : VA)	−132758
MF(BCC_A2&FE; TI : VA)	$RT\ln\left(7.92\cdot10^{-7}\right)$
MQ(BCC_A2&TI; TI : VA)	−147686
MF(BCC_A2&TI; TI : VA)	$RT\ln\left(1.89\cdot10^{-7}\right)$
MQ(BCC_A2&TI; FE : VA)	−216437
MF(BCC_A2&TI; FE : VA)	$RT\ln\left(2.466\cdot10^{-4}\right)$

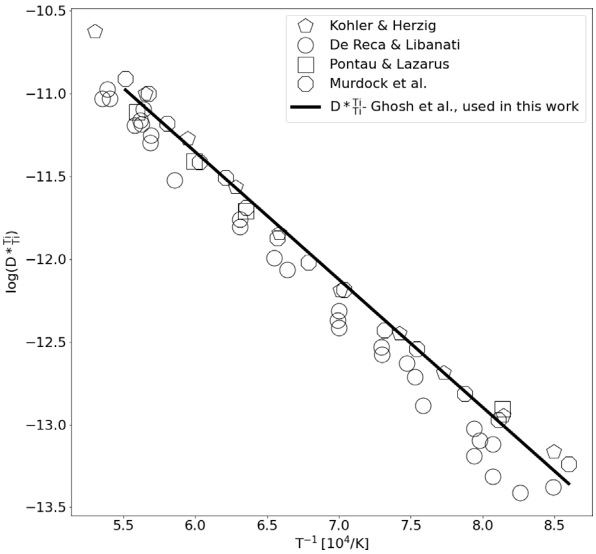

Fig. 2. Tracer diffusivity of Ti in BCC-Ti after [1,20–24].

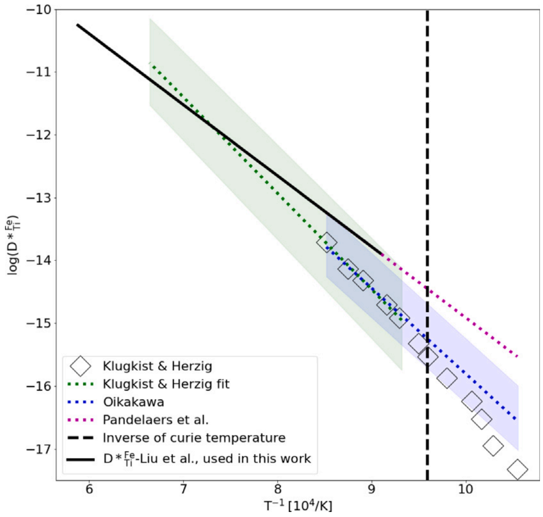

Fig. 3. Impurity diffusivity of Ti in BCC-Fe after [1,25–27].

Fig. 2 shows that the first degree fit is in good agreement with the experimental measurements of tracer diffusivity of Ti in BCC-Ti.

The Ti impurity diffusivity in Fe [1,25,26] is reviewed in Ref. [27] which was used in the present work, see Fig. 3.

3.3. Optimiser

The Thermo-Calc software package [13] contains both optimisers for assessing thermodynamic and kinetic data, and these are included in the two different PARROT modules. The DICTRA PARROT module that assesses kinetic data can use mobilities or diffusivities as input for the assessment of the mobility parameter that is stored in the kinetic databases. There are a number of limitations of the DICTRA PARROT module, where the main one is that the data used in the optimisation has usually been obtained by the use of a Matano analysis. This results in a loss of information and makes it difficult to estimate the accuracy of the optimisation. It is also challenging to optimise parameters from different alloy systems simultaneously.

Table 2
Assessed Ti-FeTi,Fe-FeTi ternary interactions.

MQ(BCC_A2&TI; FE; TI : VA; 0)	−513800
MF(BCC_A2&TI; FE; TI : VA; 0)	$199.3\cdot T$
MQ(BCC_A2&FE; FE; TI : VA; 0)	−450100
MF(BCC_A2&FE; FE; TI : VA; 0)	$301.5\cdot T$

In DICTRA, a sub-module has therefore been implemented to remedy these limitations [28]. This tool makes it possible to directly use the information obtained from the composition profiles of the diffusion couples. Using this method, it is also possible to use information from multicomponent diffusion couples to assess mobilities in lower order systems.

For the optimisation process, a DICTRA simulation setup that only includes the disordered BCC phase was used. A mixed boundary condition consisting of a fixed activity of Fe and zero flux of Ti was set up to emulate the interface between the FeTi intermetallic phase and the disordered BCC; in a binary system under isobarothermal conditions, the activities at the phase interface are constant.

4. Results

FAST effectively consolidated the Fe powder above the already solid Ti, creating Ti-Fe diffusion couples with clean interfaces. Fig. 4 shows the diffusion zone of Fe into Ti, consisting of different microstructural layers depending on Fe concentration. Firstly, there is a thin intermetallic layer at the boundary (approx 4 μm thick), expected to consist of TiFe and $TiFe_2$. This is followed by BCC-Ti, stabilised by Fe in the solid solution. The HCP Ti phase then begins to precipitate out as the Fe content is no longer sufficient to fully stabilise the BCC phase, leading to a dual phase HCP + BCC microstructure seen in alloys such as Ti-6Al-4V. The ratio of HCP:BCC continues to increase with distance from the boundary until only HCP phase remains. Fe has essentially no solubility in the HCP phase; therefore, this is an excellent visual aid in estimating the total diffusion distance. Some porosity is present in the Fe region close to the interface in the 1273 K couple but not in the 1173 K one. This suggests that its presence is not due to incomplete sintering; rather, it is due to the Kirkendall effect. Kirkendall porosity can appear due to the higher diffusion rate of Fe in Ti compared to the one of Ti in Fe, and Fe self-diffusion [29], causing vacancy accumulation.

The microstructures formed are dependent on the cooling rate, with the Ti-Fe equilibrium phase diagram (Fig. 6) showing that the BCC phase of Ti is metastable at room temperature and that HCP + TiFe phases will form under equilibrium conditions. This phase formation did not occur after FAST processing, as a sufficient cooling rate of $\approx 100\,\mathrm{K/min}$ that occurs when the electrical current is stopped, retains the BCC phase. The same conditions apply to the heating step.

EPMA analysis gave data for high resolution Fe concentration profiles across the boundaries in Fig. 4. Fig. 5 shows how the Fe concentration changes across the full scan line. A sudden decrease is observed across the interface, followed by a gradual decline across the BCC region. The Fe content then becomes irregular at the HCP + BCC region, as the intensity is dependent on which phase the measurement is taken at each point.

The optimised interaction parameters using the endmembers from Table 1 are listed in Table 2.

Simulation results of Fe impurity diffusion in Ti at 1173 K for 60 min using the optimised interaction parameters is shown in Figs. 7 and 8

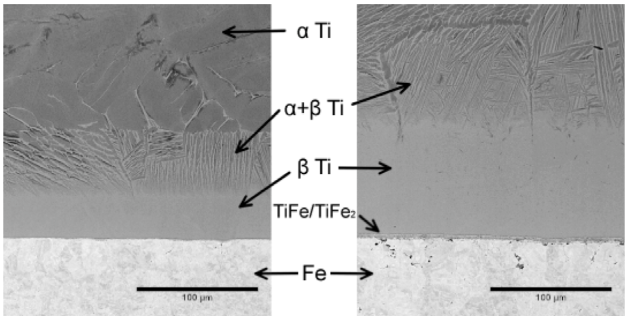

Fig. 4. SEM micrographs (BSE) of Ti-Fe diffusion couples processed for 60 min at 1173 K (left) and 1273 K (right), α is Ti-HCP, β is BCC-Ti, TiFe/TiFe$_2$ are intermetallic phases.

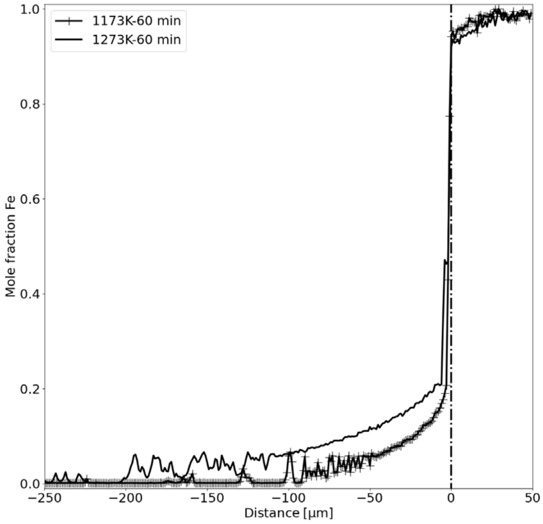

Fig. 5. EPMA measurement of Fe concentration profile in Ti-Fe diffusion couples heat treated at 1173 and 1273 K for 60 min.

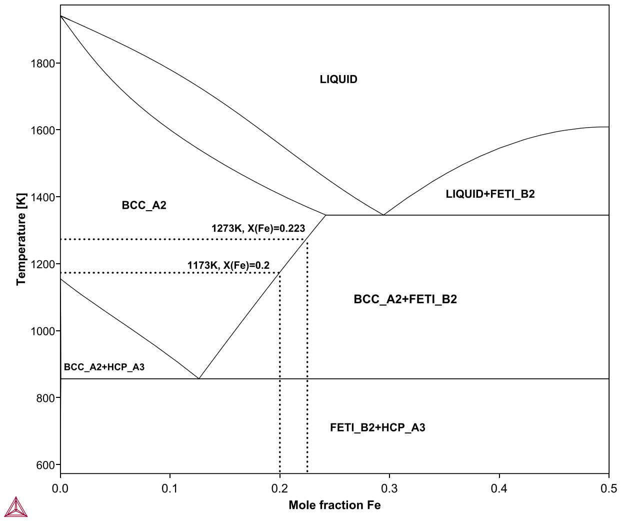

Fig. 6. Ti-Fe phase diagram. Iso activity line in BCC-Ti, FeTi two phase region at 1173 K and 1273 K determines the equilibrium composition of the interface between ordered and disordered BCC-Ti.

alongside the experimental data points obtained from EPMA Fig. 5. The boundary condition of the simulation domain models the interface between the FeTi inter-metallic phase and the disordered BCC. After

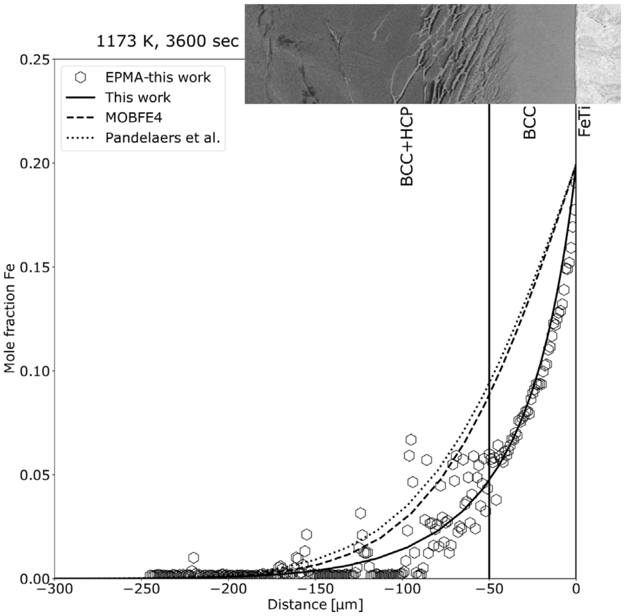

Fig. 7. Modelled and measured concentration profile of Fe in Ti-Fe diffusion couple heat treated at 1173 K, for 60 min.

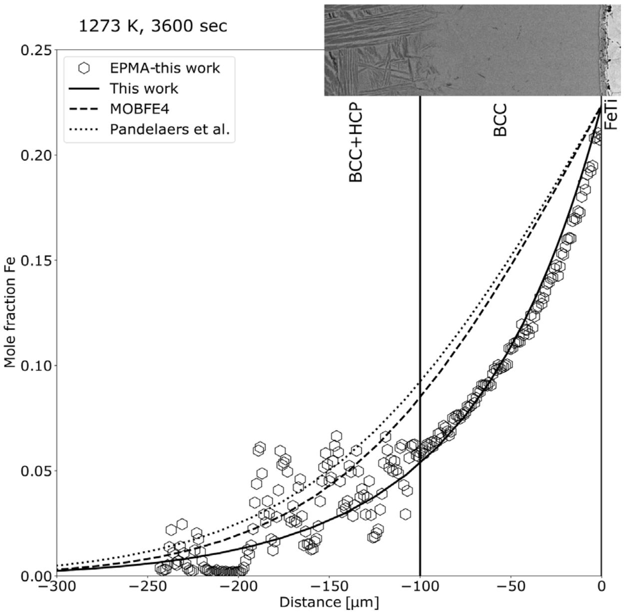

Fig. 8. Modelled and measured concentration profile of Fe in Ti-Fe diffusion couple heat treated at 1273 K, for 60 min.

60 min heat treatment at 1173 K, the thickness of the disordered BCC phase of the Ti region is $\sim 50\ \mu m$, see Figs. 4, 7 and 8.

The thickness of the disordered BCC-Ti layer is $\sim 100\ \mu m$ at 1273 K. Scattered experimental points at the left hand side of the disordered BCC are in the BCC, HCP two phase region. In this region concentration of Fe fluctuates depending on the phase area which the electron beam goes through. A low concentration indicates the HCP phase and a high concentration BCC.

The agreement between the experimental observations and simulations with the optimised parameters are shown in Figs. 7 and 8. Results of the same simulation with previous optimisations of the interaction parameters [1,2] underestimate the concentration profile.

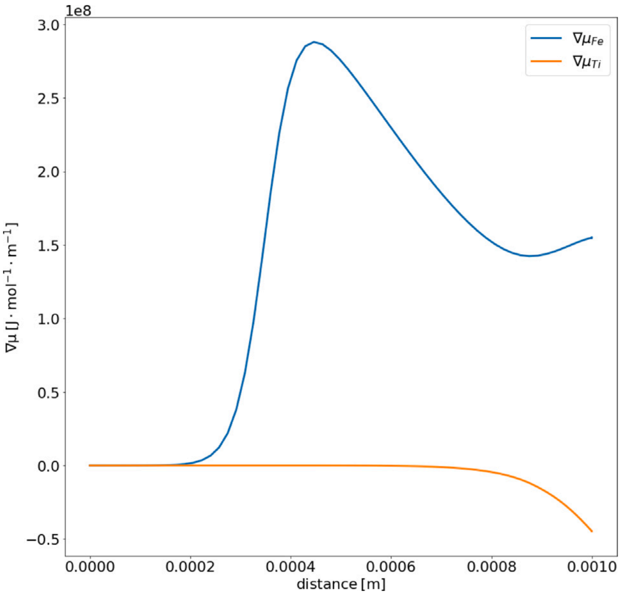

Fig. 9. Simulated gradients of chemical potentials of Fe and Ti at 1273 K from in the last timestep (TCFE9 database).

5. Conclusions and discussion

Ti powder was consolidated into pellets via field assisted sintering then reinserted in a graphite mould with Fe powder for 1 h at 1173 K and 1273 K. The diffusion profile of Fe in disordered BCC were analysed by electron probe microanalysis (EPMA) across the interfaces and for backscattered electron (BSE) scanning electron microscopy. BSE micrographs showed how Fe diffusion into the Ti caused stabilisation of the BCC phase, with a gradual change in microstructure observed across the diffusion zone. Greater diffusion was seen in the diffusion couple processed at 1273 K, with a layer of retained BCC phase measuring approximately 100 μm compared to just 50 μm when processed at 1173 K. The concentration profiles for these regions were then used to optimise the mobilities.

The use of the profile optimisation module within DICTRA makes it possible to optimise kinetic parameters flexibly and ensures that no relevant information has been lost in obtaining the parameters.

Interaction mobility parameters of Ti-Fe and Fe-Ti in disordered BCC are optimised from EPMA experimental data and assessed tracer diffusivity of Fe, Tracer diffusivity of Ti, and impurity diffusivity of Ti in Fe and Fe in Ti from literature, by using the profile optimisation module within DICTRA.

Results of the optimisation are incorporated into a mobility database, and diffusion of Fe in disordered BCC phase of Ti at 1173 K and 1273 K for 1 h are modelled using the optimised mobilities, and TCFE9 thermodynamic database [30]. Modelled profiles using optimised mobilities showed a better agreement with the experimental composition profile obtained by EPMA on diffusion couples in comparison to the results of simulations with mobility databases from previous studies.

Unlike the binary interactions, which have a dependency on the thermodynamic description of the system, the self and tracer mobilities do not depend on which thermodynamic description is used Section 3.1. Fig. 9 shows simulated gradients of chemical potentials of iron and titanium during the last timestep of the simulation at 1273 K (calculated by TCFE9 database). These gradients are driving the diffusion process in the simulations.

Declaration of competing interest

The authors declare that they have no known competing financial interests or personal relationships that could have appeared to influence the work reported in this paper.

Data availability

The authors declare that all of the data used in this research and produced during this work are included in this manuscript.

Acknowledgements

This work was partly funded by the Swedish Foundation for Strategic Research (SSF), Sweden, contract RMA15-0062. We acknowledge Sandvik Coromant, Sandvik Mining and Rock Technology and Seco Tools for support. The authors would like to thank Henry Royce Institute for Advanced Materials, EPSRC, United Kingdom grants EP/R00661X/1, EP/S019367/1, EP/P02470X/1 and EP/P025285/1, EP/L016257/1, for access to the FCT Systeme HP D 25 SPS furnace. D Guan also would like to thank the UKRI, United Kingdom for his Future Leaders Fellowship, MR/T019123/1.

References

[1] L. Pandelaers, B. Blanpain, P. Wollants, An optimized diffusion database for the disordered and ordered bcc phases in the binary Fe–Ti system, CALPHAD 35 (4) (2011) 518–522.

[2] Thermo-Calc Software MOBFE Steels/Fe-alloys mobility database version 4, 2020, (Accessed 8 February 2020).

[3] N. Weston, B. Thomas, M. Jackson, Processing metal powders via field assisted sintering technology (FAST): a critical review, Mater. Sci. Technol. 35 (11) (2019) 1306–1328.

[4] J.J. Pope, E.L. Calvert, N.S. Weston, M. Jackson, FAST-DB: a novel solid-state approach for diffusion bonding dissimilar titanium alloy powders for next generation critical components, J. Mater Process. Technol. 269 (2019) 200–207.

[5] A. Mitchell, A. Kawakami, S. Cockcroft, Beta fleck and segregation in titanium alloy ingots, High Temp. Mater. Process. 25 (5–6) (2006) 337–349.

[6] H. Nakajima, S. Ohshida, K. Nonaka, Y. Yoshida, F. Fujita, Diffusion of iron in {beta} Ti-Fe alloys, Scr. Mater. 34 (6) (1996).

[7] P.D. Hartung, B. Kramer, B. Von Turkovich, Tool wear in titanium machining, CIRP Ann. 31 (1) (1982) 75–80.

[8] C. Ramirez, A.I. Ismail, C. Gendarme, M. Dehmas, E. Aeby-Gautier, G. Poulachon, F. Rossi, Understanding the diffusion wear mechanisms of WC-10% Co carbide tools during dry machining of titanium alloys, Wear 390 (2017) 61–70.

[9] O. Hatt, Z. Lomas, M. Thomas, M. Jackson, The effect of titanium alloy chemistry on machining induced tool crater wear characteristics, Wear 408 (2018) 200–207.

[10] L. Bolzoni, Low-cost Fe-bearing powder metallurgy Ti alloys, Metal Powder Rep. 74 (6) (2019) 308–313.

[11] J. Umeda, T. Tanaka, T. Teramae, S. Kariya, J. Fujita, H. Nishikawa, Y. Shibutani, J. Shen, K. Kondoh, Microstructures analysis and quantitative strengthening evaluation of powder metallurgy Ti–Fe binary extruded alloys with (α+β)-dual-phase, Mater. Sci. Eng. A 803 (2021) 140708.

[12] S. Graham, L. Benson, M. Jackson, Direct electrochemical production of pseudo-binary Ti–Fe alloys from mixtures of synthetic rutile and iron(III) oxide, J. Mater. Sci. 55 (2020) 15988–16001.

[13] J.-O. Andersson, T. Helander, L. Höglund, P. Shi, B. Sundman, Thermo-Calc & DICTRA, computational tools for materials science, CALPHAD 26 (2) (2002) 273–312.

[14] B. Jönsson, On ferromagnetic ordering and lattice diffusion: a simple model, Z. Met.kd. 83 (5) (1992) 349–355.

[15] B. Jönsson, Assessment of the mobilities of Cr, Fe and Ni in bcc Cr-Fe-Ni alloys, ISIJ Int. 35 (11) (1995) 1415–1421.

[16] H. Lukas, S.G. Fries, B. Sundman, Computational Thermodynamics: The Calphad Method, Cambridge University Press, 2007.

[17] L.G. Kurneluk, L.M. Mirsky, B.S. Bokshtein, Investigation of lattice defects, electric structure, and diffusion mobility in titanium, in: R.I. Jaffee, H.M. Burte (Eds.), Titanium Science and Technology: Proceedings of the Second International Conference Organized by the Metallurgical Society of AIME, Vol. 2, Kresge Auditorium, Massachusetts Institute of Technology, Plenum, Cambridge, Massachusetts, 1973, p. 905.

[18] R. Peart, D. Tomlin, Diffusion of solute elements in beta-titanium, Acta Metall. 10 (2) (1962) 123–134.

[19] G. Gibbs, D. Graham, D. Tomlin, Diffusion in titanium and titanium—niobium alloys, Phil. Mag. 8 (92) (1963) 1269–1282.

[20] G. Ghosh, Thermodynamic and kinetic modeling of the Cr-Ti-V system, J. Phase Equilib. 23 (4) (2002) 310–328.

[21] A.E. Pontau, D. Lazarus, Diffusion of titanium and niobium in bcc Ti-Nb alloys, Phys. Rev. B 19 (8) (1979) 4027.

[22] J. Murdock, T. Lundy, E. Stansbury, Diffusion of Ti44 and V48 in titanium, Acta Metall. 12 (9) (1964) 1033–1039.

[23] U. Köhler, C. Herzig, On the anomalous self-diffusion in BCC titanium, Phys. Status Solidi b 144 (1) (1987) 243–251.

[24] N.W. De Reca, et al., Autodifusion de titanio beta y hafnio beta, Acta Metall. 16 (10) (1968) 1297–1305.

[25] H. Oikawa, Lattice diffusion in iron-a review, Tetsu Hagane 68 (10) (1982) 1489–1497.

[26] P. Klugkist, C. Herzig, Tracer diffusion of titanium in α-iron, Phys. Status Solidi a 148 (2) (1995) 413–421.

[27] Y. Liu, L. Zhang, Y. Du, D. Liang, Ferromagnetic ordering and mobility end-members for impurity diffusion in bcc Fe, CALPHAD 33 (4) (2009) 732–736.

[28] L. Höglund, unpublished work, 2021.

[29] F. Seitz, On the porosity observed in the Kirkendall effect, Acta Metall. (ISSN: 0001-6160) 1 (3) (1953) 355–369.

[30] Thermo-Calc Software TCFE Steels/Fe-alloys thermodynamic database version 9, 2020, (Accessed 8 February 2020).